



## Atmospheric Chemistry and Physics

### Introduction to the European Monitoring and Evaluation Programme (EMEP) and observed atmospheric composition change during 1972–2009

K. Tørseth, W. Aas, K. Breivik, A. M. Fjæraa, M. Fiebig, A. G. Hjellbrekke, C. Lund Myhre, S. Solberg, and K. E. Yttri  
NILU – Norwegian Institute for Air Research, Kjeller, Norway

#### Abstract

European scale harmonized monitoring of atmospheric composition was initiated in the early 1970s, and the activity has generated a comprehensive dataset (available at <http://www.emep.int>) which allows the evaluation of regional and spatial trends of air pollution during a period of nearly 40 years. Results from the monitoring made within EMEP, the European Monitoring and Evaluation Programme, show large reductions in ambient concentrations and deposition of sulphur species during the last decades. Reductions are in the order of 70–90% since the year 1980, and correspond well with reported emission changes. Also reduction in emissions of nitrogen oxides ( $\text{NO}_x$ ) are reflected in the measurements, with an average decrease of nitrogen dioxide and nitrate in precipitation by about 23% and 25% respectively since 1990. Only minor reductions are however seen since the late 1990s. The concentrations of total nitrate in air have decreased on average only by 8% since 1990, and fewer sites show a significant trend. A majority of the EMEP sites show a decreasing trend in reduced nitrogen both in air and precipitation on the order of 25% since 1990. Deposition of base cations has decreased during the past 30 years, and the pH in precipitation has increased across Europe. Large inter annual variations in the particulate matter mass concentrations reflect meteorological variability, but still there is a relatively clear overall decrease at several sites during the last decade. With few observations going back to the 1990s, the observed chemical composition is applied to document a change in particulate matter (PM) mass even since 1980. These data indicate an overall reduction of about  $5 \mu\text{g}/\text{m}^3$  from sulphate alone. Despite the significant reductions in sulphur emissions, sulphate still remains one of the single most important compounds contributing to regional scale aerosol mass concentration. Long-term ozone trends at EMEP sites show a mixed pattern. The

year-to-year variability in ozone due to varying meteorological conditions is substantial, making it hard to separate the trends caused by emission change from other effects. For the Nordic countries the data indicate a reduced occurrence of very low concentrations. The most pronounced change in the frequency distribution is seen at sites in the UK and the Netherlands, showing a reduction in the higher values. Smaller changes are seen in Germany, while in Switzerland and Austria, no change is seen in the frequency distribution of ozone. The lack of long-term data series is a major obstacle for studying trends in volatile organic compounds (VOC). The scatter in the data is large, and significant changes are only found for certain components and stations. Concentrations of the heavy metals lead and cadmium have decreased in both air and precipitation during the last 20 years, with reductions in the order of 80–90% for Pb and 64–84% for Cd (precipitation and air respectively). The measurements of total gaseous mercury indicate a dramatic decrease in concentrations during 1980 to about 1993. Trends in hexachlorocyclohexanes (HCHs) show a significant decrease in annual average air concentrations. For other persistent organic pollutants (POPs) the patterns is mixed, and differs between sites and between measurements in air versus precipitation.

#### Reference

Tørseth, K. et al. (2012): [Introduction to the European Monitoring and Evaluation Programme \(EMEP\) and observed atmospheric composition change during 1972–2009](#), *Atmos. Chem. Phys.*, 12, 5447–5481

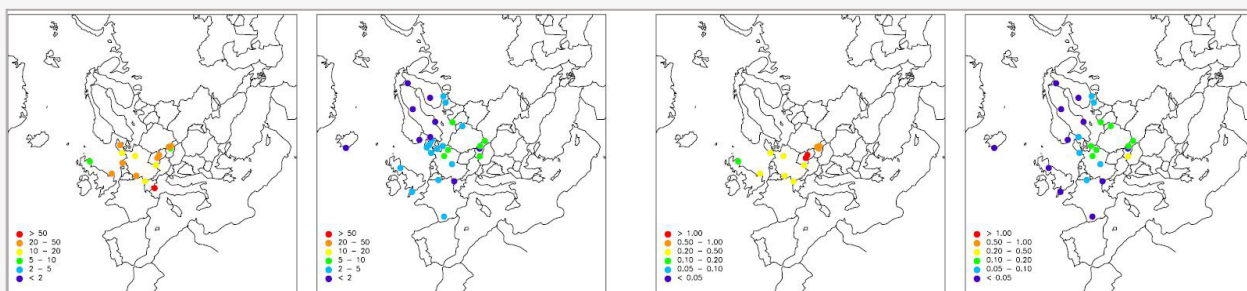
### Summer ammonia measurements in a densely populated Mediterranean city

M. Pandolfi<sup>1</sup>, F. Amato<sup>2</sup>, C. Reche<sup>1</sup>, A. Alastuey<sup>1</sup>, R. P. Otjes<sup>3</sup>, M. J. Blom<sup>3</sup>, and X. Querol<sup>1</sup>

<sup>1</sup>Inst. of Environmental Assessment and Water Research, Barcelona, Spain

<sup>2</sup>TNO, Built Environment and Geosciences, Dept. of Air Quality and Climate, Utrecht, The Netherlands

<sup>3</sup>Energy Research Centre of the Netherlands, Department of Environmental Assessment, Petten, The Netherlands



Left panels: Average concentrations of Pb in aerosols in 1990 and 2009 in  $\text{ng Pb m}^{-3}$ ; Right panels: Average concentrations of Cd in aerosols in 1990 and 2009 in  $\text{ng Cd m}^{-3}$ . (From Tørseth, K. et al, 2012)

### Abstract

Real-time measurements of ambient concentrations of gas-phase ammonia ( $\text{NH}_3$ ) were performed in Barcelona (NE Spain) in summer between May and September 2011. Two measurement sites were selected: one in an urban background traffic-influenced area (UB) and the other in the historical city centre (CC). Levels of  $\text{NH}_3$  were higher at CC ( $5.6 \pm 2.1 \mu\text{g m}^{-3}$  or  $7.5 \pm 2.8$  ppbv) compared with UB ( $2.2 \pm 1.0 \mu\text{g m}^{-3}$  or  $2.9 \pm 1.3$  ppbv). This difference is attributed to the contribution from non-traffic sources such as waste containers, sewage systems, humans and open markets more dense in the densely populated historical city centre. Under high temperatures in summer these sources had the potential to increase the ambient levels of  $\text{NH}_3$  well above the urban-background-traffic-influenced UB measurement station. Measurements were used to assess major local emissions, sinks and diurnal evolution of  $\text{NH}_3$ . The measured levels of  $\text{NH}_3$ , especially high in the old city, may contribute to the high mean annual concentrations of secondary sulfate and nitrate measured in Barcelona compared with other cities in Spain affected

by high traffic intensity. Ancillary measurements, including PM<sub>10</sub>, PM<sub>2.5</sub>, PM<sub>1</sub> levels (Particulate Matter with aerodynamic diameter smaller than 10  $\mu\text{m}$ , 2.5  $\mu\text{m}$ , and 1  $\mu\text{m}$ ), gases and black carbon concentrations and meteorological data, were performed during the measurement campaign. The analysis of specific periods (three special cases) during the campaign revealed that road traffic was a significant source of  $\text{NH}_3$ . However, its effect was more evident at UB compared with CC where it was masked given the high levels of  $\text{NH}_3$  from non-traffic sources measured in the old city. The relationship between  $\text{SO}_4^{2-}$  daily concentrations and gas-fraction ammonia ( $\text{NH}_3/(\text{NH}_3 + \text{NH}_4^+)$ ) revealed that the gas-to-particle phase partitioning (volatilization or ammonium salts formation) also played an important role in the evolution of  $\text{NH}_3$  concentration in summer in Barcelona.

### Reference

Pandolfi, M. et al. (2012): [Summer ammonia measurements in a densely populated Mediterranean city](#), *Atmos. Chem. Phys.*, 12, 7557–7575

## Atmospheric Measurement Techniques

### Comparison of OH concentration measurements by DOAS and LIF during SAPHIR chamber experiments at high OH reactivity and low NO concentration

H. Fuchs, H.-P. Dorn, M. Bachner, B. Bohn, T. Brauers, S. Gomm, A. Hofzumahaus, F. Holland, S. Nehr, F. Rohrer, R. Tillmann, and A. Wahner  
*Institute of Energy and Climate Research, IEK-8: Troposphere, Forschungszentrum Jülich GmbH, Germany*

### Abstract

During recent field campaigns, hydroxyl radical (OH) concentrations that were measured by laser-induced fluorescence (LIF) were up to a factor of ten larger than predicted by current chemical models for conditions of high OH reactivity and low NO concentration. These discrepancies, which were observed in forests and urban-influenced rural environments, are so far not entirely understood. In summer 2011, a series of experiments was carried out in the atmosphere simulation chamber SAPHIR in Jülich, Germany, in order to investigate the photochemical degradation of isoprene, methyl-vinyl ketone (MVK), methacrolein (MACR) and aromatic compounds by OH. Conditions were similar to those experienced during the PRIDE-PRD2006 campaign in the Pearl River Delta (PRD), China, in 2006, where a large difference between OH measurements and model predictions was found. During experiments in SAPHIR, OH was simultaneously detected by two independent instruments: LIF and differential optical absorption spectroscopy (DOAS). Because DOAS is an inherently calibration-free technique, DOAS measurements are regarded as a reference standard. The comparison of the two techniques was used to investigate potential artifacts in the LIF measurements for PRD-like conditions of OH reactivities of 10 to 30  $\text{s}^{-1}$  and NO mixing ratios of 0.1 to 0.3 ppbv. The analysis of twenty experiment days shows good agreement. The linear regression of the combined data set (averaged to the DOAS time resolution, 2495

data points) yields a slope of  $1.02 \pm 0.01$  with an intercept of  $(0.10 \pm 0.03) \times 10^6 \text{ cm}^{-3}$  and a linear correlation coefficient of  $R^2 = 0.86$ . This indicates that the sensitivity of the LIF instrument is well-defined by its calibration procedure. No hints for artifacts are observed for isoprene, MACR, and different aromatic compounds. LIF measurements were approximately 30–40% (median) larger than those by DOAS after MVK (20 ppbv) and toluene (90 ppbv) had been added. However, this discrepancy has a large uncertainty and requires further laboratory investigation. Observed differences between LIF and DOAS measurements are far too small to explain the unexpected high OH concentrations during the PRIDE-PRD2006 campaign.

### Reference

Fuchs, H. et al. (2012): [Comparison of OH concentration measurements by DOAS and LIF during SAPHIR chamber experiments at high OH reactivity and low NO concentration](#), *Atmos. Meas. Tech.*, 5, 1611–1626

### Aerosol information content analysis of multi-angle high spectral resolution measurements and its benefit for high accuracy greenhouse gas retrievals

C. Frankenberg<sup>1</sup>, O. Hasekamp<sup>2</sup>, C. O'Dell<sup>3</sup>, S. Sanghavi<sup>1</sup>, A. Butz<sup>4</sup>, and J. Worden<sup>1</sup>

<sup>1</sup>Jet Propulsion Lab, California Institute of Technology, Pasadena, USA

<sup>2</sup>SRON Netherlands Institute for Space Research, Utrecht, The Netherlands

<sup>3</sup>Colorado State University, Fort Collins, USA

<sup>4</sup>Karlsruhe Institute of Technology, IMK-ASF, Karlsruhe, Germany

### Abstract

New generations of space-borne spectrometers for the retrieval of atmospheric abundances of greenhouse gases require unprecedented accuracies as atmospheric variability of long-lived gases is very low. These instruments, such as GOSAT and OCO-2, typically



Artist Rendition of the Orbiting Carbon Observatory, OCO-2 (Credit: John Howard/JPL)

use a high spectral resolution oxygen channel ( $O_2$  A-band) in addition to  $CO_2$  and  $CH_4$  channels to discriminate changes in the photon path-length distribution from actual trace gas amount changes. Inaccurate knowledge of the photon path-length distribution, determined

by scatterers in the atmosphere, is the prime source of systematic biases in the retrieval. In this paper, we investigate the combined aerosol and greenhouse gas retrieval using multiple satellite viewing angles simultaneously. We find that this method, hitherto only applied in multi-angle imagery such as from POLDER or MISR, greatly enhances the ability to retrieve aerosol properties by 2–3 degrees of freedom. We find that the improved capability to retrieve aerosol parameters significantly reduces interference errors introduced into retrieved  $CO_2$  and  $CH_4$  total column averages. Instead of focussing solely on improvements in spectral and spatial resolution, signal-to-noise ratios or sampling frequency, multiple angles reduce uncertainty in space based greenhouse gas retrievals more effectively and provide a new potential for dedicated aerosols retrievals.

#### Reference

Frankenberg, C. et al. (2012): [Aerosol information content analysis of multi-angle high spectral resolution measurements and its benefit for high accuracy greenhouse gas retrievals](#), *Atmos. Meas. Tech.*, 5, 1809–1821

## Biogeosciences

2509–2522

### Detecting anthropogenic carbon dioxide uptake and ocean acidification in the North Atlantic Ocean

N. R. Bates<sup>1</sup>, M. H. P. Best<sup>1</sup>, K. Neely<sup>1</sup>, R. Garley<sup>1</sup>,  
A. G. Dickson<sup>2</sup>, and R. J. Johnson<sup>1</sup>

<sup>1</sup>Bermuda Institute of Ocean Sciences, Ferry Reach, Bermuda

<sup>2</sup>Scripps Institution of Oceanography, Uni. of California San Diego, USA

#### Abstract

Fossil fuel use, cement manufacture and land-use changes are the primary sources of anthropogenic carbon dioxide ( $CO_2$ ) to the atmosphere, with the ocean absorbing approximately 30% (Sabine et al., 2004). Ocean uptake and chemical equilibration of anthropogenic  $CO_2$  with seawater results in a gradual reduction in seawater pH and saturation states ( $\Omega$ ) for calcium carbonate ( $CaCO_3$ ) minerals in a process termed ocean acidification. Assessing the present and future impact of ocean acidification on marine ecosystems requires detection of the multi-decadal rate of change across ocean basins and at ocean time-series sites. Here, we show the longest continuous record of ocean  $CO_2$  changes and ocean acidification in the North Atlantic subtropical gyre near Bermuda from 1983–2011. Dissolved inorganic carbon (DIC) and partial pressure of  $CO_2$  ( $pCO_2$ ) increased in surface seawater by  $\sim 40 \mu mol kg^{-1}$  and  $\sim 50 \mu atm$  ( $\sim 20\%$ ), respectively. Increasing Revelle factor ( $\beta$ ) values imply that the capacity of North Atlantic surface waters to absorb  $CO_2$  has also diminished. As indicators of ocean acidification, seawater pH decreased by  $\sim 0.05$  ( $0.0017 yr^{-1}$ ) and  $\omega$  values by  $\sim 7$ – $8\%$ . Such data provide critically needed multi-decadal information for assessing the North Atlantic Ocean  $CO_2$  sink and the pH changes that determine marine ecosystem responses to ocean acidification.

#### Reference

Bates, N. R. et al. (2012): [Detecting anthropogenic carbon dioxide uptake and ocean acidification in the North Atlantic Ocean](#), *Biogeosciences*, 9,

### A synthesis of carbon in international trade

G. P. Peters<sup>1</sup>, S. J. Davis<sup>2,3</sup>, and R. Andrew<sup>1</sup>

<sup>1</sup>Center for International and Environmental Research Oslo, Norway

<sup>2</sup>Dept. of Global Ecology, Carnegie Institution of Washington, Stanford, USA

<sup>3</sup>Dept. of Earth System Science, University of California, Irvine, USA

#### Abstract

In a globalized world, the transfer of carbon between regions, either physically or embodied in production, represents a substantial fraction of global carbon emissions. The resulting emission transfers are important for balancing regional carbon budgets and for understanding the drivers of emissions. In this paper we synthesize current understanding in two parts: (1)  $CO_2$  emissions embodied in goods and services that are produced in one country but consumed in others, and (2) carbon physically present in fossil fuels, petroleum-derived products, harvested wood products, crops, and livestock products. We describe the key differences between studies and provide a consistent set of estimates using the same definitions, modelling framework, and consistent data. We find the largest trade flows of carbon in international trade in 2004 were fossil fuels (2673 MtC, 37% of global emissions),  $CO_2$  embodied in traded goods and services (1661 MtC, 22% of global emissions), crops (522 MtC, 31% of total harvested crop carbon), petroleum-based products (183 MtC, 50% of their total production), harvested wood products (149 MtC, 40% of total roundwood extraction), and livestock products (28 MtC, 22% of total livestock carbon). We find that for embodied  $CO_2$  emissions, estimates from independent studies are robust, and that differences between individual studies are not a reflection of the uncertainty in consumption-based estimates, but rather these differences result from the use of different production-based emissions input data and different definitions for allocating emissions to international trade. After adjusting for these issues, results across independent studies converge to give less uncertainty than previously

assumed. For physical carbon flows there are relatively few studies to be synthesized, but differences between existing studies are due to the method of allocating to international trade, with some studies using 'apparent consumption' as opposed to 'final consumption'. While results across studies are sufficiently robust to be used in further applications, more research is needed to understand differences and to harmonize definitions for particular applications.

#### Reference

Peters, G. P., Davis, S. J., and Andrew, R. (2012): [A synthesis of carbon in international trade](#), *Biogeosciences*, 9, 3247–3276

## Novel water source for endolithic life in the hyperarid core of the Atacama Desert

J. Wierzchos<sup>1</sup>, A. F. Davila<sup>2</sup>, I. M. Sánchez-Almazo<sup>3</sup>, M. Hajnos<sup>4</sup>, R. Swieboda<sup>5</sup>, and C. Ascaso<sup>1</sup>

<sup>1</sup>Museo Nacional de Ciencias Naturales, MNCN-CSIC, Madrid, Spain

<sup>2</sup>NASA Ames Research Center, Moffett Field, USA

<sup>3</sup>Universidad de Granada CIC, Granada, Spain

<sup>4</sup>Institute of Agrophysics PAN, Lublin, Poland

<sup>5</sup>Medical University of Lublin, Lublin, Poland

#### Abstract

The hyperarid core of the Atacama Desert, Chile, is possibly the driest and most life-limited place on Earth, yet endolithic microorganisms thrive inside halite pinnacles that are part of ancient salt flats. The existence of this microbial community in an environment that excludes any other life forms suggests biological adaptation to high salinity and desiccation stress, and indicates an alternative source of water for life other than rainfall, fog or dew. Here, we show that halite endoliths obtain liquid water through spontaneous capillary condensation at relative humidity (RH) much lower than the deliquescence RH of NaCl. We describe how this condensation could occur inside nano-pores smaller than 100 nm, in a newly characterized halite phase that is intimately associated with the endolithic aggregates. This nano-porous phase helps retain liquid water for long periods of time by preventing its evaporation even in conditions of utmost dryness. Our results explain how life has colonized and adapted to one of the most extreme environments on our planet, expanding the water activity envelope for life on Earth, and broadening the spectrum of possible habitats for life beyond our planet.

#### Reference

Wierzchos, J. et al. (2012): [Novel water source for endolithic life in the hyperarid core of the Atacama Desert](#), *Biogeosciences*, 9, 2275–2286



The Atacama in northern Chile is the driest desert in the world (Credit: ESO)

## Bioerosion by euendoliths decreases in phosphate-enriched skeletons of living corals

C. Godinot<sup>1</sup>, A. Tribollet<sup>2</sup>, R. Grover<sup>1</sup>, and C. Ferrier-Pagès<sup>1</sup>

<sup>1</sup>Centre Scientifique de Monaco, CSM, Monaco

<sup>2</sup>Institut de Recherche pour le Développement, UMR IPSL-LOCEAN (IRD/CNRS/UPMC/MNH), Bondy, France

#### Abstract

While the role of microboring organisms, or euendoliths, is relatively well known in dead coral skeletons, their function in live corals remains poorly understood. They are suggested to behave like ectosymbionts or parasites, impacting their host's health. However, the species composition of microboring communities, their abundance and dynamics in live corals under various environmental conditions have never been explored. Here, the effect of phosphate enrichment on boring microorganisms in live corals was tested for the first time. *Stylophora pistillata* nubbins were exposed to three different treatments (phosphate concentrations of 0, 0.5 and 2.5  $\mu\text{mol l}^{-1}$ ) during 15 weeks. After 15 weeks of phosphate enrichment, petrographic thin sections were prepared for observation with light microscopy, and additional samples were examined with scanning electron microscopy (SEM). Euendoliths comprised mainly phototrophic *Ostreobium sp.* filaments. Rare filaments of heterotrophic fungi were also observed. Filaments were densely distributed in the central part of nubbins, and less abundant towards the apex. Unexpectedly, there was a visible reduction of filament abundance in the most recently calcified apical part of phosphate-enriched nubbins. The overall abundance of euendoliths significantly decreased, from  $9.12 \pm 1.09\%$  of the skeletal surface area in unenriched corals, to  $5.81 \pm 0.77\%$  and  $5.27 \pm 0.34\%$  in 0.5 and 2.5  $\mu\text{mol l}^{-1}$ -phosphate enriched corals respectively. SEM observations confirmed this decrease. Recent studies have shown that phosphate enrichment increases coral skeletal growth and metabolic rates, while it decreases skeletal density and resilience to mechanical stress. We thus hypothesize that increased skeletal growth in the presence of phosphate enrichment occurred too fast for an effective expansion of euendolith growth. They could not keep up with coral growth, so they became diluted in the apex areas as nubbins grew with phosphate enrichment. Results from the present study suggest that coral skeletons of *S. pistillata* will not be further weakened by euendoliths under phosphate enrichment.

#### Reference

Godinot, C. et al. (2012): [Bioerosion by euendoliths decreases in phosphate-enriched skeletons of living corals](#), *Biogeosciences*, 9, 2377–2384

## Organic matter dynamics and stable isotope signature as tracers of the sources of suspended sediment

Y. Schindler Wildhaber, R. Liechti, and C. Alewell

Institute for Environmental Geosciences, Basel, Switzerland

#### Abstract

Suspended sediment (SS) and organic matter in rivers can harm brown trout *Salmo trutta* by affecting the health and fitness of free

swimming fish and by causing siltation of the riverbed. The temporal and spatial dynamics of sediment, carbon (C), and nitrogen (N) during the brown trout spawning season in a small river of the Swiss Plateau were assessed and C isotopes as well as the C/N atomic ratio were used to distinguish autochthonous and allochthonous sources of organic matter in SS loads. The visual basic programme *IsoSource* with  $^{13}\text{C}_{\text{tot}}$  and  $^{15}\text{N}$  as input isotopes was used to quantify the temporal and spatial sources of SS. Organic matter concentrations in the infiltrated and suspended sediment were highest during low flow periods with small sediment loads and lowest during high flow periods with high sediment loads. Peak values in nitrate and dissolved organic C were measured during high flow and high rainfall, probably due to leaching from pasture and arable land. The organic matter was of allochthonous sources as indicated by the C/N atomic ratio and  $\delta^{13}\text{C}_{\text{org}}$ . Organic matter in SS increased from up- to downstream due to an increase of pasture and arable land downstream of the river. The mean fraction of SS originating from upper watershed riverbed sediment decreased from up to downstream and increased during high flow at all measuring sites along the course of the river. During base flow conditions, the major sources of SS are pasture, forest and arable land. The latter increased during rainy and warmer winter periods, most likely because both triggered snow melt and thus erosion. The measured increase in DOC and nitrate concentrations during high flow support these modelling results. Enhanced soil erosion processes on pasture and arable land are expected with increasing heavy rain events and less snow during winter seasons due to climate change. Consequently, SS and organic matter in the river will increase, which will possibly affect brown trout negatively.

#### Reference

Schindler Wildhaber, Y., Liechti, R., and Alewell, C. (2012): [Organic matter dynamics and stable isotope signature as tracers of the sources of suspended sediment](#), *Biogeosciences*, 9, 1985–1996

## Photoproduction of ammonium in the southeastern Beaufort Sea and its biogeochemical implications

H. Xie<sup>1</sup>, S. Bélanger<sup>2</sup>, G. Song<sup>1</sup>, R. Benner<sup>3</sup>, A. Taalba<sup>1</sup>, M. Blais<sup>4</sup>, J.-É. Tremblay<sup>4</sup>, and M. Babin<sup>4,5</sup>

<sup>1</sup>Institut des Sciences de la Mer, Uni. du Québec à Rimouski, Canada

<sup>2</sup>Dépt. Biologie, Chimie et Géographie, Uni. du Québec à Rimouski, Canada

<sup>3</sup>University of South Carolina, Columbia, USA

<sup>4</sup>Dépt. Biologie, Québec-Océan and Takuvik, Université Laval, Canada

<sup>5</sup>Lab. d'Océanographie de Villefranche, CNRS & Univ. Pierre et Marie Curie, France

#### Abstract

Photochemistry of dissolved organic matter (DOM) plays an important role in marine biogeochemical cycles, including the regeneration of inorganic nutrients. DOM photochemistry affects nitrogen cycling by converting bio-refractory dissolved organic nitrogen to labile inorganic nitrogen, mainly ammonium ( $\text{NH}_4^+$ ). During the August 2009 Mackenzie Light and Carbon (MALINA) Program, the absorbed photon-based efficiency spectra of  $\text{NH}_4^+$  photoproduction (i.e. photoammonification) were determined using water samples from the SE Beaufort Sea, including the Mackenzie River estuary, shelf, and Canada Basin. The photoammonification efficiency decreased with increasing wavelength across the ultraviolet and

visible regimes and was higher in offshore waters than in shelf and estuarine waters. The efficiency was positively correlated with the molar nitrogen:carbon ratio of DOM and negatively correlated with the absorption coefficient of chromophoric DOM (CDOM). Combined with collateral measurements of  $\text{CO}_2$  and CO photoproduction, this study revealed a stoichiometry of DOM photochemistry with a  $\text{CO}_2 : \text{CO} : \text{NH}_4^+$  molar ratio of 165 : 11 : 1 in the estuary, 60 : 3 : 1 on the shelf, and 18 : 2 : 1 in the Canada Basin. The  $\text{NH}_4^+$  efficiency spectra, along with solar photon fluxes, CDOM absorption coefficients and sea ice concentrations, were used to model the monthly surface and depth-integrated photoammonification rates in 2009. The summertime (June–August) rates at the surface reached  $6.6 \text{ nmol l}^{-1} \text{ d}^{-1}$  on the Mackenzie Shelf and  $3.7 \text{ nmol l}^{-1} \text{ d}^{-1}$  further offshore; the depth-integrated rates were correspondingly  $8.8 \text{ } \mu\text{mol m}^{-2} \text{ d}^{-1}$  and  $11.3 \text{ } \mu\text{mol m}^{-2} \text{ d}^{-1}$ . The offshore depth-integrated rate in August ( $8.0 \text{ } \mu\text{mol m}^{-2} \text{ d}^{-1}$ ) was comparable to the missing dissolved inorganic nitrogen (DIN) source required to support the observed primary production in the upper 10-m layer of that area. The yearly  $\text{NH}_4^+$  photoproduction in the entire study area was estimated to be  $1.4 \times 10^8$  moles, with 85% of it being generated in summer when riverine DIN input is low. Photoammonification could mineralize 4% of the annual dissolved organic nitrogen (DON) exported from the Mackenzie River and provide a DIN source corresponding to 7% of the riverine DIN discharge and 1400 times the riverine  $\text{NH}_4^+$  flux. Under a climate warming-induced ice-free scenario, these quantities could increase correspondingly to 6%, 11%, and 2100 times. Photoammonification is thus a significant nitrogen cycling term and may fuel previously unrecognized autotrophic and heterotrophic production pathways in the surface SE Beaufort Sea.

#### Reference

Xie, H. et al. (2012): [Photoproduction of ammonium in the southeastern Beaufort Sea and its biogeochemical implications](#), *Biogeosciences*, 9, 3047–3061

## Towards a merged satellite and in situ fluorescence ocean chlorophyll product

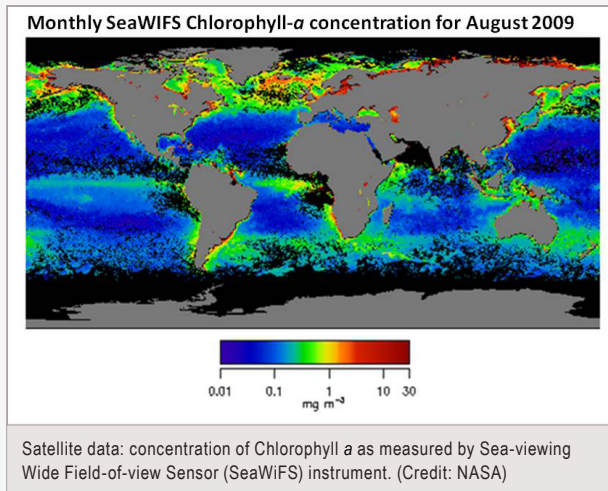
H. Lavigne<sup>1,2</sup>, F. D'Ortenzio<sup>1,2</sup>, H. Claustre<sup>1,2</sup>, and A. Poteau<sup>1,2</sup>

<sup>1</sup>Laboratoire d'Océanographie de Villefranche, CNRS, France

<sup>2</sup>Université Pierre et Marie Curie-Paris 6, Laboratoire d'Océanographie de Villefranche, France

#### Abstract

Understanding the ocean carbon cycle requires a precise assessment of phytoplankton biomass in the oceans. In terms of numbers of observations, satellite data represent the largest available data set. However, as they are limited to surface waters, they have to be merged with in situ observations. Amongst the in situ data, fluorescence profiles constitute the greatest data set available, because fluorometers have operated routinely on oceanographic cruises since the 1970s. Nevertheless, fluorescence is only a proxy of the total chlorophyll *a* concentration and a data calibration is required. Calibration issues are, however, sources of uncertainty, and they have prevented a systematic and wide range exploitation of the fluorescence data set. In particular, very few attempts to standardize the fluorescence databases have been made. Consequently, merged estimations with other data sources (e.g. satellite) are lacking.



We propose a merging method to fill this gap. It consists firstly in adjusting the fluorescence profile to impose a zero chlorophyll  $a$  concentration at depth. Secondly, each point of the fluorescence profile is then multiplied by a correction coefficient, which forces the chlorophyll  $a$  integrated content measured on the fluorescence profile to be consistent with the concomitant ocean colour observation. The method is close to the approach proposed by Boss et al. (2008) to correct fluorescence data of a profiling float, although important

differences do exist. To develop and test our approach, in situ data from three open ocean stations (BATS, HOT and DYFAMED) were used. Comparison of the so-called 'satellite-corrected' fluorescence profiles with concomitant bottle-derived estimations of chlorophyll  $a$  concentration was performed to evaluate the final error (estimated at 31%). Comparison with the Boss et al. (2008) method, using a subset of the DYFAMED data set, demonstrated that the methods have similar accuracy. The method was applied to two different data sets to demonstrate its utility. Using fluorescence profiles at BATS, we show that the integration of 'satellite-corrected' fluorescence profiles in chlorophyll  $a$  climatologies could improve both the statistical relevance of chlorophyll  $a$  averages and the vertical structure of the chlorophyll  $a$  field. We also show that our method could be efficiently used to process, within near-real time, profiles obtained by a fluorometer deployed on autonomous platforms, in our case a bio-optical profiling float. The application of the proposed method should provide a first step towards the generation of a merged satellite/fluorescence chlorophyll  $a$  product, as the 'satellite-corrected' profiles should then be consistent with satellite observations. Improved climatologies with more consistent satellite and in situ data are likely to enhance the performance of present biogeochemical models.

#### Reference

Lavigne, H. et al. (2012): [Towards a merged satellite and in situ fluorescence ocean chlorophyll product](#), *Biogeosciences*, 9, 2111–2125

## Hydrology and Earth System Sciences

### Climatic and geologic controls on suspended sediment flux in the Sutlej River Valley, western Himalaya

H. Wulf<sup>1</sup>\*, B. Bookhagen<sup>2</sup>, and D. Scherler<sup>1</sup>

<sup>1</sup>Department of Earth and Environmental Science, Potsdam Uni., Germany

<sup>2</sup>Department of Geography, University of California, Santa Barbara, USA

\*now at: Remote Sensing Section, Helmholtz Centre Potsdam, GFZ German Research Center for Geosciences, Germany

#### Abstract

The sediment flux through Himalayan rivers directly impacts water quality and is important for sustaining agriculture as well as maintaining drinking-water and hydropower generation. Despite the recent increase in demand for these resources, little is known about the triggers and sources of extreme sediment flux events, which lower water quality and account for extensive hydropower reservoir filling and turbine abrasion. Here, we present a comprehensive analysis of the spatiotemporal trends in suspended sediment flux based on daily data during the past decade (2001–2009) from four sites along the Sutlej River and from four of its main tributaries. In conjunction with satellite data depicting rainfall and snow cover, air temperature and earthquake records, and field observations, we infer climatic and geologic controls of peak suspended sediment concentration

(SSC) events. Our study identifies three key findings: First, peak SSC events ( $\geq 99^{\text{th}}$  SSC percentile) coincide frequently (57–80%) with heavy rainstorms and account for about 30% of the suspended sediment flux in the semi-arid to arid interior of the orogen. Second, we observe an increase of suspended sediment flux from the Tibetan Plateau to the Himalayan Front at mean annual timescales. This sediment-flux gradient suggests that averaged, modern erosion in the western Himalaya is most pronounced at frontal regions, which are characterized by high monsoonal rainfall and thick soil cover. Third, in seven of eight catchments, we find an anticlockwise hysteresis loop of annual sediment flux variations with respect to river discharge, which appears to be related to enhanced glacial sediment evacuation during late summer. Our analysis emphasizes the importance of unconsolidated sediments in the high-elevation sector that can easily be mobilized by hydrometeorological events and higher glacial-meltwater contributions. In future climate change scenarios, including continuous glacial retreat and more frequent monsoonal rainstorms across the Himalaya, we expect an increase in peak SSC events, which will decrease the water quality and impact hydropower generation.

#### Reference

Wulf, H., Bookhagen, B., and Scherler, D. (2012): [Climatic and geologic controls on suspended sediment flux in the Sutlej River Valley, western Himalaya](#), *Hydrol. Earth Syst. Sci.*, 16, 2193–2217

## Value of medium range weather forecasts in the improvement of seasonal hydrologic prediction skill

S. Shukla<sup>1</sup>, N. Voisin<sup>2</sup>, and D. P. Lettenmaier<sup>1</sup>

<sup>1</sup>Department of Civil and Environmental Engineering, University of Washington, Seattle, USA

<sup>2</sup>Pacific Northwest National Laboratory, Richland, USA

### Abstract

We investigated the contribution of medium range weather forecasts with lead times of up to 14 days to seasonal hydrologic prediction skill over the conterminous United States (CONUS). Three different Ensemble Streamflow Prediction (ESP) based experiments were performed for the period 1980–2003 using the Variable Infiltration Capacity (VIC) hydrology model to generate forecasts of monthly runoff and soil moisture (SM) at lead-1 (first month of the forecast period) to lead-3. The first experiment (ESP) used a resampling from the retrospective period 1980–2003 and represented full climatological uncertainty for the entire forecast period. In the second and third experiments, the first 14 days of each ESP ensemble

member were replaced by either observations (perfect 14-day forecast) or by a deterministic 14-day weather forecast. We used Spearman rank correlations of forecasts and observations as the forecast skill score. We estimated the potential and actual improvement in baseline skill as the difference between the skill of experiments 2 and 3 relative to ESP, respectively. We found that useful runoff and SM forecast skill at lead-1 to -3 months can be obtained by exploiting medium range weather forecast skill in conjunction with the skill derived by the knowledge of initial hydrologic conditions. Potential improvement in baseline skill by using medium range weather forecasts for runoff [SM] forecasts generally varies from 0 to 0.8 [0 to 0.5] as measured by differences in correlations, with actual improvement generally from 0 to 0.8 of the potential improvement. With some exceptions, most of the improvement in runoff is for lead-1 forecasts, although some improvement in SM was achieved at lead-2.

### Reference

Shukla, S., Voisin, N., and Lettenmaier, D. P. (2012): [Value of medium range weather forecasts in the improvement of seasonal hydrologic prediction skill](#), *Hydrol. Earth Syst. Sci.*, 16, 2825–2838

## Natural Hazards and Earth System Sciences

### Building an 18,000-year-long paleo-earthquake record from detailed deep-sea turbidite characterization in Poverty Bay, New Zealand

H. Poudoux<sup>1,2</sup>, G. Lamarche<sup>2</sup>, and J.-N. Proust<sup>1</sup>

<sup>1</sup>Géosciences-Rennes, Université de Rennes 1, France

<sup>2</sup>National Institute of Water and Atmospheric Research (NIWA) Ltd, Wellington, New Zealand

### Abstract

Two ~20-m-long sedimentary cores collected in two neighbouring mid-slope basins of the Paritu Turbidite System in Poverty Bay, east of New Zealand, show a high concentration of turbidites (5 to 6 turbidites per meter), interlaid with hemipelagites, tephra and a few debris. Turbidites occur as both stacked and single, and exhibit a range of facies from muddy to sandy turbidites. The age of each turbidite is estimated using the statistical approach developed in the OxCal software from an exceptionally dense set of tephrochronology and radiocarbon ages (~1 age per meter). The age, together with the facies and the petrophysical properties of the sediment (density, magnetic susceptibility and P-wave velocity), allows the correlation of turbidites across the continental slope (1400–2300 m water depth). We identify 73 synchronous turbidites, named basin events, across the two cores between  $819 \pm 191$  and  $17\,729 \pm 701$  yr BP. Compositional, foraminiferal and geochemical signatures of the turbidites are used to characterize the source area of the sediment, the origin of the turbidity currents, and their triggering mechanism. Sixty-seven basin events are interpreted as originated from slope failures on the upper continental slope in water depth ranging from 150 to 1200 m. Their earthquake trigger is inferred from the heavily gullied morphology of the source area and the water depth at which slope failures originated. We derive an earthquake



Earthquakes in New Zealand are common since the country is part of the Pacific Ring of Fire, which is geologically active. Poverty Bay is one of several bays on the east coast of the North Island. (Credit: NASA)

mean return time of ~230 yr, with a 90% probability range from 10 to 570 yr. The earthquake chronology indicates cycles of progressive decrease of earthquake return times from ~400 yr to ~150 yr at 0–7 kyr, 8.2–13.5 kyr, 14.7–18 kyr. The two 1.2 kyr-long intervals in between (7–8.2 kyr and 13.5–14.7 kyr) correspond to basin-wide reorganizations with anomalous turbidite deposition (finer deposits and/or non-deposition) reflecting the emplacement of two large mass transport deposits much more voluminous than the ‘classical’ earthquake-triggered turbidites. Our results show that the progressive characterization of a turbidite record from a single sedimentary system can provide a continuous paleo-earthquake history in regions of short historical record and incomplete onland paleo-earthquake evidences. The systematic description of each turbidite enables us to infer the triggering mechanism.

## Reference

Pouderoux, H., Lamarche, G., and Proust, J.-N. (2012): [Building an 18,000-year-long paleo-earthquake record from detailed deep-sea turbidite characterization in Poverty Bay, New Zealand](#), *Nat. Hazards Earth Syst. Sci.*, 12, 2077–2101

## The spatial structure of European wind storms as characterized by bivariate extreme-value Copulas

A. Bonazzi, S. Cusack, C. Mitas, and S. Jewson  
*Risk Management Solutions, Peninsular House, London, UK*

### Abstract

The winds associated with extra-tropical cyclones are amongst the costliest natural perils in Europe. Re/insurance companies typically have insured exposure at multiple locations and hence the losses they incur from any individual storm crucially depend on that storm's spatial structure. Motivated by this, this study investigates the spatial structure of the most extreme windstorms in Europe. The data consists of a carefully constructed set of 135 of the most damaging storms in the period 1972–2010. Extreme value copulas are applied to this data to investigate the spatial dependencies of gusts.

The copula method is used to investigate three aspects of windstorms. First, spatial maps of expected hazard damage between large cities and their surrounding areas are presented. Second, we demonstrate a practical application of the copula method to benchmark catalogues of artificial storms for use in the re/insurance sector. Third, the copula-based method is used to investigate the sensitivity of spatially aggregated damage to climate variability. The copula method allows changes to be expressed in terms of storm frequency, local intensity, and storm spatial structure and gives a more detailed view of how climate variability may affect multi-location risk in Europe.

### Reference

Bonazzi, A. et al. (2012): [The spatial structure of European wind storms as characterized by bivariate extreme-value Copulas](#), *Nat. Hazards Earth Syst. Sci.*, 12, 1769–1782

## Enhancing flood resilience through improved risk communications

J. J. O'Sullivan<sup>1</sup>, R. A. Bradford<sup>1</sup>, M. Bonaiuto<sup>2</sup>, S. De Dominicis<sup>2</sup>, P. Rotko<sup>3</sup>, J. Aaltonen<sup>3</sup>, K. Waylen<sup>4</sup>, and S. J. Langan<sup>4</sup>

<sup>1</sup>University College Dublin, Ireland

<sup>2</sup>Sapienza Università di Roma, Rome, Italy

<sup>3</sup>Finnish Environment Institute, Helsinki, Finland

<sup>4</sup>The James Hutton Institute, Aberdeen, Scotland

### Abstract

A framework of guiding recommendations for effective pre-flood and flood warning communications derived from the URFlood project (2<sup>nd</sup> ERA-Net CRUE Research Funding Initiative) from extensive quantitative and qualitative research in Finland, Ireland, Italy and Scotland is presented. Eleven case studies in fluvial, pluvial, coastal, residual, and 'new' flood risk locations were undertaken.

The recommendations were developed from questionnaire surveys by exploring statistical correlations of actions and understandings of individuals in flood risk situations to low, moderate and high resilience groupings. Groupings were based on a conceptual relationship of self-assessed levels of awareness, preparedness and worry. Focus groups and structured interviews were used to discuss barriers in flood communications, explore implementation of the recommendations and to rank the recommendations in order of perceived importance. Results indicate that the information deficit model for flood communications that relies on the provision of more and better information to mitigate risk in flood-prone areas is insufficient, and that the communications process is very much multi-dimensional. The recommendations are aimed at addressing this complexity and their careful implementation is likely to improve the penetration of flood communications. The recommendations are applicable to other risks and are transferable to jurisdictions beyond the project countries.

### Reference

O'Sullivan, J. J. et al. (2012): [Enhancing flood resilience through improved risk communications](#), *Nat. Hazards Earth Syst. Sci.*, 12, 2271–2282

## Severe wind gust thresholds for Meteoalarm derived from uniform return periods in ECA&D

A. Stepek, I. L. Wijnant, G. van der Schrier, E. J. M. van den Besselaar, and A. M. G. Klein Tank  
*Climate Services Dept, KNMI, De Bilt, The Netherlands*

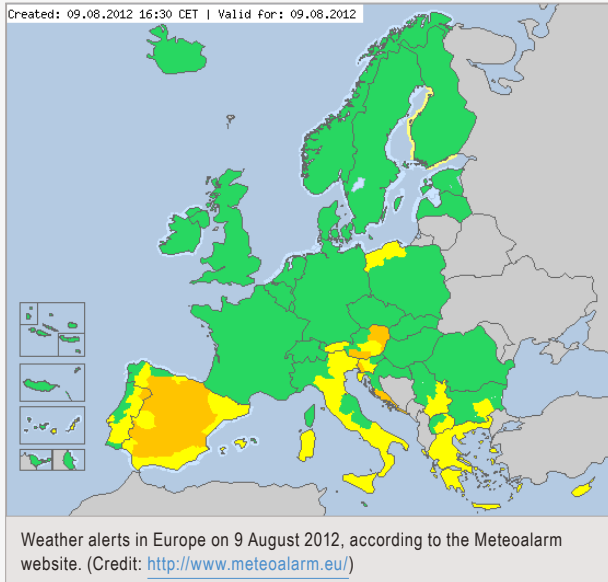
### Abstract

In this study we present an alternative wind gust warning guideline for Meteoalarm, the severe weather warning website for Europe. There are unrealistically large differences in levels and issuing frequencies of all warning levels currently in use between neighbouring Meteoalarm countries. This study provides a guide for the Meteoalarm community to review their wind gust warning thresholds. A more uniform warning system is achieved by using one pan-European return period per warning level. The associated return values will be different throughout Europe because they depend on local climate conditions, but they will not change abruptly at country borders as is currently the case for the thresholds. As return values are a measure of the possible danger of an event and its impact on society, they form an ideal basis for a warning system. Validated wind gust measurements from the European Climate Assessment and Dataset (ECA&D, <http://www.ecad.eu>) were used to calculate return values of the annual maximum wind gust. The current thresholds are compared with return values for 3 different return periods: 10 times a year return periods for yellow warnings, 2 yr periods for orange and 5 yr periods for red warnings. So far 10 countries provide wind gust data to ECA&D. Due to the ECA&D completeness requirements and the fact that some countries provided too few stations to be representative for that country, medians of the return values of annual maximum wind gust could be calculated for 6 of the 10 countries. Alternative guideline thresholds are presented for Norway, Ireland, The Netherlands, Germany, the Czech Republic, and Spain and the need to distinguish between coastal, inland and mountainous regions is demonstrated. The new thresholds based on uniform return periods differ significantly from the current ones, particularly for coastal and mountainous areas.

We are aware of other, sometimes binding factors (e.g. laws) that prevent participating counties from implementing this climatology based warning system.

### Reference

Stepek, A. et al. (2012): [Severe wind gust thresholds for Meteoalarm derived from uniform return periods in ECA&D](#), *Nat. Hazards Earth Syst. Sci.*, 12, 1969–1981



### Risk perception – issues for flood management in Europe

R. A. Bradford<sup>1</sup>, J. J. O'Sullivan<sup>1</sup>, I. M. van der Craats<sup>2</sup>, J. Krywkow<sup>3</sup>, P. Rotko<sup>4</sup>, J. Aaltonen<sup>4</sup>, M. Bonaiuto<sup>5</sup>, S. De Dominicis<sup>5</sup>, K. Waylen<sup>6</sup>, and K. Schelfaut<sup>2,7</sup>

<sup>1</sup>Centre for Water Resources Research, University College Dublin, Ireland

<sup>2</sup>Antea Group, Gent, Belgium

<sup>3</sup>Seeconsult GmbH, Osnabruck, Germany

<sup>4</sup>Suomen Ymparistokeskus (Finnish Environment Institute), Helsinki, Finland

<sup>5</sup>Sapienza Università di Roma, Rome, Italy

<sup>6</sup>James Hutton Institute, Aberdeen, Scotland, UK

<sup>7</sup>University of Ghent, Vakgroep Geografie, Gent, Belgium

### Abstract

Public perception of flood risk and flood risk information is often overlooked when developing flood risk management plans. As scientists and the public at large perceive risk in very different ways, flood risk management strategies are known to have failed in the past due to this disconnect between authorities and the public. This paper uses a novel approach in exploring the role of public perception in developing flood risk communication strategies in Europe. Results are presented of extensive quantitative research of 1375 questionnaire responses from thirteen communities at risk across six European countries. The research forms part of two research projects funded under the 2<sup>nd</sup> ERA-Net CRUE Funding Initiative: URflood and FREEMAN. Risk perception is conceptualized as a pillar of social resilience, representing an innovative approach to the

issue. From this process recommendations are identified for improving flood risk management plans through public participation.

### Reference

Bradford, R. A. et al. (2012): [Risk perception – issues for flood management in Europe](#), *Nat. Hazards Earth Syst. Sci.*, 12, 2299–2309

### Searching for the seafloor signature of the 21 May 2003 Boumerdès earthquake offshore central Algeria

A. Cattaneo<sup>1</sup>, N. Babonneau<sup>2</sup>, G. Ratzov<sup>2</sup>, G. Dan-Unterseh<sup>2\*</sup>, K. Yelles<sup>3</sup>, R. Bracène<sup>4</sup>, B. Mercier de Lépinay<sup>5</sup>, A. Boudiaf<sup>6</sup>, and J. Déverchère<sup>2</sup>

<sup>1</sup>Ifremer, GM-LES, Plouzané, France

<sup>2</sup>Université de Brest, IUEM-CNRS Domaines Océaniques, Plouzané, France

<sup>3</sup>CRAAG, Algiers, Algeria

<sup>4</sup>SONATRACH, Division Exploration, Boumerdès, Algeria

<sup>5</sup>Géosciences Azur, CNRS, Valbonne, France

<sup>6</sup>Université des Sciences Montpellier 2, Sète, France

\*now at: FUGRO FRANCE S.A.S., Nanterre, France

### Abstract

Shaking by moderate to large earthquakes in the Mediterranean Sea has proved in the past to potentially trigger catastrophic sediment collapse and flow. On 21 May 2003, a magnitude 6.8 earthquake located near Boumerdès (central Algerian coast) triggered large turbidity currents responsible for 29 submarine cable breaks at the foot of the continental slope over ~150 km from west to east. Seafloor bathymetry and backscatter imagery show the potential imprints of the 2003 event and of previous events. Large slope scarps resulting from active deformation may locally enhance sediment instabilities, although faults are not directly visible at the seafloor. Erosion is evident at the foot of the margin and along the paths of the numerous canyons and valleys. Cable breaks are located at the outlets of submarine valleys and in areas of turbidite levee over-spilling and demonstrate the multi-source and multi-path character of the 2003 turbidite event. Rough estimates of turbidity flow velocity are not straightforward because of the multiple breaks along the same cable, but seem compatible with those measured in other submarine cable break studies elsewhere.

While the signature of the turbidity currents is mostly erosional on the continental slope, turbidite beds alternating with hemipelagites accumulate in the distal reaches of sediment dispersal systems. In perspective, more chronological work on distal turbidite successions offshore Algeria offers promising perspectives for paleoseismology reconstructions based on turbidite dating, if synchronous turbidites along independent sedimentary dispersal systems are found to support triggering by major earthquakes. Preliminary results on sediment core PSM-KS23 off Boumerdès typically show a 800-yr interval between turbidites during the Holocene, in accordance with the estimated mean seismic cycle on land, even if at this stage it is not yet possible to prove the earthquake origin of all the turbidites.

### Reference

Cattaneo, A. et al. (2012): [Searching for the seafloor signature of the 21 May 2003 Boumerdès earthquake offshore central Algeria](#), *Nat. Hazards Earth Syst. Sci.*, 12, 2159–2172

## Impact of heat and drought stress on arable crop production in Belgium

A. Gobin

Flemish Institute for Technological Research (VITO), Belgium

### Abstract

Modelling approaches are needed to accelerate understanding of adverse weather impacts on crop performances and yields. The aim was to elicit biometeorological conditions that affect Belgian arable crop yield, commensurate with the scale of climatic impacts. The regional crop model REGCROP (Gobin, 2010) enabled to examine changing weather patterns in relation to the crop season and crop

sensitive stages of six arable crops: winter wheat, winter barley, winter rapeseed, potato, sugar beet and maize. The sum of vapour pressure deficit during the growing season is the single best predictor of arable yields, with  $R^2$  ranging from 0.55 for sugar beet to 0.76 for wheat. Drought and heat stress, in particular during the sensitive crop stages, occur at different times in the crop season and significantly differ between two climatic periods, 1947–1987 and 1988–2008. Though average yields have risen steadily between 1947 and 2008, there is no evidence that relative tolerance to stress has improved.

### Reference

Gobin, A. (2012): [Impact of heat and drought stress on arable crop production in Belgium](#), *Nat. Hazards Earth Syst. Sci.*, 12, 1911–1922

# The Cryosphere

## Statistical adaptation of ALADIN RCM outputs over the French Alps – application to future climate and snow cover

M. Rousselot, Y. Durand, G. Giraud, L. Mérindol, I. Dombrowski-Etchevers, M. Déqué, and H. Castebrunet  
Météo-France/CNRS, Grenoble, France

### Abstract

In this study, snowpack scenarios are modelled across the French Alps using dynamically downscaled variables from the ALADIN Regional Climate Model (RCM) for the control period (1961–1990) and three emission scenarios (SRES B1, A1B and A2) for the mid- and late 21<sup>st</sup> century (2021–2050 and 2071–2100). These variables are statistically adapted to the different elevations, aspects and slopes of the Alpine massifs. For this purpose, we use a simple analogue criterion with ERA40 series as well as an existing detailed climatology of the French Alps (Durand et al., 2009a) that provides complete meteorological fields from the SAFRAN analysis model. The resulting scenarios of precipitation, temperature, wind, cloudiness, longwave and shortwave radiation, and humidity are used to run the physical snow model CROCUS and simulate snowpack evolution over the massifs studied. The seasonal and regional characteristics of the simulated climate and snow cover changes are explored, as is the influence of the scenarios on these changes. Preliminary results suggest that the snow water equivalent (SWE) of the snowpack will decrease dramatically in the next century, especially in the Southern and Extreme Southern parts of the Alps. This decrease seems to result primarily from a general warming throughout the year, and possibly a deficit of precipitation in the autumn. The magnitude of the snow cover decline follows a marked altitudinal gradient, with the highest altitudes being less exposed to climate change. Scenario A2, with its high concentrations of greenhouse gases, results in a SWE reduction roughly twice as large as in the low-emission scenario B1 by the end of the century. This study needs to be completed using simulations from other RCMs, since a multi-model approach is essential for uncertainty analysis.

### Reference

Rousselot, M. et al. (2012): [Statistical adaptation of ALADIN RCM outputs over the French Alps – application to future climate and snow cover](#), *The Cryosphere*, 6, 785–805

## Extrapolating glacier mass balance to the mountain-range scale: the European Alps 1900–2100

M. Huss

Department of Geosciences, University of Fribourg, Switzerland

### Abstract

This study addresses the extrapolation of in-situ glacier mass balance measurements to the mountain-range scale and aims at deriving time series of area-averaged mass balance and ice volume change for all glaciers in the European Alps for the period 1900–2100. Long-term mass balance series for 50 Swiss glaciers based on a combination of field data and modelling, and WGMS data for glaciers in Austria, France and Italy are used. A complete glacier inventory is available for the year 2003. Mass balance extrapolation is performed based on (1) arithmetic averaging, (2) glacier hypsometry, and (3) multiple regression. Given a sufficient number of data series, multiple regression with variables describing glacier geometry performs best in reproducing observed spatial mass balance variability. Future mass changes are calculated by driving a combined model for mass balance and glacier geometry with GCM ensembles based on four emission scenarios. Mean glacier mass balance in the European Alps is  $-0.31 \pm 0.04$  m w.e.  $a^{-1}$  in 1900–2011, and  $-1$  m w.e.  $a^{-1}$  over the last decade. Total ice volume change since 1900 is  $-96 \pm 13$  km<sup>3</sup>; annual values vary between  $-5.9$  km<sup>3</sup> (1947) and  $+3.9$  km<sup>3</sup> (1977). Mean mass balances are expected to be around  $-1.3$  m w.e.  $a^{-1}$  by 2050. Model results indicate a glacier area reduction of 4–18% relative to 2003 for the end of the 21<sup>st</sup> century.

### Reference

Huss, M. (2012): [Extrapolating glacier mass balance to the mountain-range scale: the European Alps 1900–2100](#), *The Cryosphere*, 6, 713–727